Available online at www.sciencedirect.com

SCIENCE DIRECT®

Coastal Engineering 52 (2005) 727–744

Coastal Engineering
An International Journal for Coastal, Harbour and Offshore Engineers

www.elsevier.com/locate/coastaleng

Extended equilibrium beach profiles

Wojciech Romańczyk [a,*], Barbara Boczar-Karakiewicz [a], Jerry L. Bona [b]

[a] *Université du Québec, Institut des Sciences de la Mer de Rimouski (ISMER), 310, alleé des Ursulines, Rimouski, QC, Canada, G5L 3A1*
[b] *University of Illinois at Chicago, Department of Mathematics, Statistics and Computer Science, Chicago, IL 60607, U.S.A.*

Received 12 August 2003; received in revised form 28 April 2005; accepted 20 May 2005
Available online 24 June 2005

Abstract

The idea of an equilibrium beach profile has been a useful concept in both theoretical and practical coastal engineering studies. In essence, the subject has thus far evolved to a choice of shape functions, which are described by a small set of parameters. Additional efforts have attempted to relate these parameters to more fundamental quantities, such as average grain size of the bottom sediment, wave environment, geometric aspects of the beach, and the like. This approach has a long history and can rightly claim a certain level of success. However, the usual collections of shape functions are well-known to have difficulties very near the shoreline, let alone on the nearshore portion of the beach. This study extends the equilibrium profile up to and somewhat past the shoreline. Three shape functions are used in conjunction with a Taylor expansion for the nearshore and above water portions of the profile. A nonlinear fitting technique is applied to estimate the model's best parameter values. Moreover, reduced versions of the proposed models can be employed for prediction based only on parameters related to sediment characteristics or wave conditions and geometry of the visible beach. The approach is compared with data from the East Coast of Australia, the East Coast of North America and the South Shore of the Mediterranean Sea.

Keywords: Beach profile; Equilibrium; Surf zone; Beach profile shape functions; Nearshore-zone geometry; Beach stability

1. Introduction

The concept of an equilibrium beach profile has been a part of the ideas in use in coastal engineering studies for at least half a century. In a two-dimensional cross-shore description, the result of various theories and concepts is a mathematical description of the form

$$h(x) = f(x, \ldots) \tag{1}$$

where x is the distance from the mean shoreline, h is the undisturbed depth of the water at the distance x offshore, and f is a shape function that depends upon, in addition to x, various properties of the nearshore zone including perhaps the bottom sediments, the wave environment, the wind environment, and the overall littoral zone geometry. Of course, one

* Corresponding author. Tel.: +1 418 724 1650; fax: +1 418 724 1842.
E-mail address: wromanczyk@yahoo.ca (W. Romańczyk).

0378-3839/$ - see front matter © 2005 Elsevier B.V. All rights reserved.
doi:10.1016/j.coastaleng.2005.05.002

may include a longshore variable, say, in the description. The existing developments, which date from the 1950s (Bruun, 1954; Dean, 1977), are well described in recent monographs (CEM, 2001; Komar, 1998; van Rijn, 1998; Silvester and Hsu, 1997) which also provide good references to older literature.

The overall concept is something like the following. In any dynamical nearshore area, there is always change occurring on smaller and perhaps intermediate scales (e.g., the formation and destruction of ripples, bar growth and migration and so on). The large scales are considered to be in equilibrium with smaller scales and they are expected to change very slowly if at all. Practically, they comprise averages wherein the smaller scales are washed out. The larger scales are expected to be determined by only the gross aspects of the local environment. The key parameters are: initial profile (slopes, height, shape), sediment characteristics (grain size, fall velocity, packing, cohesion) and hydrodynamic forces (surge level, wave height and periodicity, etc.). Of course, the latter are related to other more primitive aspects. There seem to be two main schools of thought about models representing the cross-shore beach profile. The first group based on the stability of the bottom profile as in Eq. (1), posits that erosion and accretion compensate each other (Bruun, 1954; Dean, 1977; Everts, 1978; Bodge, 1992; Komar and McDougal, 1994; Lee, 1994; Sierra et al., 1994). The second group exploits the idea that f is formed by balanced equations of sediments and shallow water equations or dispersive generalizations (Kobayashi, 1982; Watanabe, 1982; Kobayashi, 1987; Kabiling and Sato, 1993; Roelvink and Broker, 1993; Kit and Pelinovsky, 1998; Larson et al., 1999). The first group is described in more detail in Section 2.

The present work derives from the need for a description of f that can encompass both the very nearshore area and the initial portion of the onshore zone. The existing descriptions are not especially accurate in this range. We propose a mathematical artifice whereby the shape functions in present use are augmented by a one-sided Taylor expansion around a point x_0 to be described, and which is part of the existing theories. It might be objected that such a description, while likely to work because of general results about polynomial approximation, requires the determination of too many additional parameters to be practically useful. It will be shown in a range of interesting examples that very good representation may be obtained using this descriptive device with only one further parameter in addition to those already inherent in f.

2. Beach profile models

The earliest study to describe an equilibrium beach profile appears to have been carried out by Fenneman (1902). This work was followed by Bruun (1954) based on his observations of beach profiles located on the Danish Coast of the North Sea and at Mission Bay, California. Bruun showed that the smoothed bed profile can be represented by a function f, that is a pure 2-parameter power function of the form

$$f(x) = -Ax^{\rho} \tag{2}$$

where the parameter A is a dimensional coefficient and ρ is a dimensionless exponent. The orientation of the coordinate system explained later in Section 4 defines the function f to be the elevation of the seabed relative to the mean water level. In consequence, $f<0$ except on the visible beach. Bruun's idea of setting the exponent to $\rho=2/3$ was further developed by Dean (1977, 1990, 1991) who provided a rationale for this value. Kriebel et al. (1991) and Work and Dean (1991) also found that in this two-parameter power-law description, the coefficient A in Eq. (2) depends on the sediment fall velocity w in something like the form

$$A = 2.25\left(\frac{w^2}{g}\right)^{\frac{1}{3}} \tag{3}$$

where g denotes the gravity constant. The values of the parameters in Eq. (2) obtained from field observations in Dean's study using a least squares fitting procedure were the following: the ρ values ranged from less than 0.1 to 1.4 and the A values ranged from 0.0017 to 4.25 $m^{1-\rho}$ (Dean, 1977). In case the parameter ρ is fixed at 2/3 and the parameter A is the only free variable, its values were less than 0.2 $m^{1/3}$ and none were greater than 0.34 $m^{1/3}$.

In later studies, Larson (1991) proposed a different, shape function f, namely

$$f(x) = -A(x+x_s)^{\frac{2}{3}} \tag{4}$$

where the third parameter x_s denotes a horizontal distance which, according to Larson was to be obtained from field data using a least squares procedure to minimize the error induced by its choice. In this description of a two-parameter shape function, Dean's estimated value $\rho=2/3$ was taken as fixed and extra freedom is obtained via the new parameter x_s. One may think of x_s physically as making some allowance for the fact that the waterline $(x,y)=(0,0)$ is not in fact an exactly determinable location (further discussion of this point may be found in Appendix A).

Completing this line of development, we here posit a 3-parameter equilibrium profile function of the form

$$f(x) = -A(x+x_s)^{\rho} \tag{5}$$

where all three parameters A, ρ and x_s are to be obtained from a fitting procedure matching field data, either directly, or indirectly by relating A, ρ and x_s to other nearshore properties.

An exponential beach profile shape function f was later proposed by Bodge (1992) and Komar and McDougal (1994), viz.

$$f(x) = -B\left(1-e^{-kx+C}\right) \tag{6}$$

where the three coefficients B, k, and C are estimated by fitting f with observations. The coefficient B appeared to be expressible in terms of aspects of the local incident wave and bottom sediment characteristics. The coefficient k was also correlated with sediment characteristics of the beach. Indeed, the idea put forward was that k mirrors variability along the profile related to change in sediment diameter across the surf zone. The dimensionless spatial translation C is here introduced for the same reason that x_s was put into Dean's power law, to give greater flexibility and to allow for the indeterminate nature of the waterline (see again Appendix A). Field observations used by Bodge (1992) provide values of k in a range of 3×10^{-5} to 1.16×10^{-3} m^{-1}. The calculated coefficients B varied from 2.7 to 70 m.

Lee (1994) suggested that a propitious choice of the shape function f was the logarithmic form

$$f(x) = -\left[D+\frac{1}{F}\ln\left(\frac{x}{G}+1\right)\right] \tag{7}$$

where the coefficient G in the argument of the logarithm is related to the grain-size diameter of the bottom sediment and F was estimated using the wave period T via the relation $F=4\pi^2/gT^2$. The coefficient D is introduced for the same reason that x_s and C are introduced in Eq. (5) and (6). In the equilibrium profile proposed by Lee, values of the coefficient F at different sites were seen to vary from 0.5 to 0.003 m^{-1} and G varied from 1 to 30,000 m.

In the context of the data sets described in some detail in Section 3, we compare the performance of the various suggestions outlined above. It will appear that all the shape functions (5)-(7) reproduce reasonably well the observed offshore portion of the equilibrium profile with appropriate choices of their parameters. By contrast, the profile of the very nearshore zone and the beach above the mean water level are not well represented by any of these shape functions, especially for barred surf zones. It is noted that the prediction of the profile above the still water level was not the intention of any of the authors, but some work was done to improve the equilibrium profile in the very nearshore zone. For example, the problem of an infinite slope at the shoreline when applying a power function was addressed by Dean (1990) and Kriebel et al. (1991), but these findings are not capable of covering the visible beach. It was this observation that led us to propose an extension of the range of these shape functions by a one-sided Taylor expansion that matches the offshore portion of f around a chosen point x_0. While this is an obvious idea, what is not so clear is how many additional parameters are required to obtain good agreement with observations. After setting forth the idea, the theory will be applied to several examples and it will be seen that only one further parameter is needed to obtain good agreement up to and past the shoreline.

The organization of the remainder of the paper is as follows. We start with descriptions of the sites used in the analysis. The description of our scheme is then presented. Comparisons of the various theories with data from the sites described are then provided. The paper closes with a brief summary and some further discussion. Appendix B contains an indication of some of the details of the procedure introduced to carry out the proposed approximations.

3. Observational data

Three field sites are used in our development. The sites in question are on the East Coast of Australia

(Gold Coast, Queensland), the East Coast of North America (Duck, North Carolina, USA) and the South Shore of the Mediterranean Sea (Tunisia, Jerba Island). These are sites where good data sets are available. Moreover, they are exposed to rather different wave climates and are characterized by different mean morphologies. In particular, the Australian site has a fairly steep offshore mean slope, the slope at Duck is intermediate, while the Tunisian site features a mild slope.

We use two typical Australian Gold Coast bed profiles. These profiles were obtained at Billinga in the period 1966–1990 by the Gold Coast City Council. More specifically, we use profiles eta21 and eta22 in the Gold Coast Council nomenclature (Gold Coast City Council, 1990; DHL, 1970). East Coast Australian bed profiles generally contain either one or two nearshore bars. The number and location of these bars reflects the response of the bottom topography to the incident wave conditions. The wave climate in this area is characterized by frequently occurring, severe storms and a cyclic recurrence of cyclones (on the average, one every two years, see Smith and Jackson, 1990). The largest waves can reach heights of 8.5–12 m with corresponding wave periods of 14–22 s (McGrath and Patterson, 1972; Boczar-Karakiewicz and Jackson, 1990; Smith and Jackson, 1990). During the periods of storm waves and cyclones, the Gold Coast beaches are usually severely eroded. They are often restored subsequently during the mild summer swell. The average bottom slope is about 0.0148. The sediment on the beach and in the nearshore zone is composed predominately of quartzose sand with median grain diameters D_{50}=0.2 to 0.3 mm (DHL, 1970).

The North American East Coast site is located at Duck, North Carolina at the Field Research Facility (FRF) of the US Army Corps of Engineers. The site extends over 1200 m in the longshore direction. Spatial bottom bathymetry measurements were carried out monthly for about 20 years, starting in 1980, and some particular profiles were surveyed more frequently (approximately bi-weekly). The measurements were made along the entire site and extended some 1 km into the ocean (Birkemeier, 1984). These measurements show regular bed contours except for irregularities in the area close to the 600 m research pier, with one or two nearshore sand bars in evidence. Again, the number and location of bars appears to be related to changes in the observed incident wave conditions. The location of the bars vary with time in a seasonal cycle, but there are also more substantial long term variations (Romańczyk et al., 1999; Boczar-Karakiewicz et al., 2005). In the present analysis, two typical bottom profiles (#62 and #188 in the local Duck coordinate system, see Birkemeier, 1984) were chosen. These profiles are located on the far ends of the experimental site, well away from the pier. The mean bottom slope of the offshore portion of the bed profile (in water depth from 2 to 8 m) is about 0.0085. The very nearshore and the lower beach are steeper with a mean slope of some 0.016. The beach sediments in the nearshore zone are well sorted and composed of fine sand (with diameters ranging from 0.11 to 0.21 mm; Nicholls, 1998). The observed wave climate shows considerable seasonal variability. Typical winter storm waves with peak periods of some 14–15 s reach wave heights in excess of 3 m (Lippman et al., 1993; Boczar-Karakiewicz et al., 2005). Typical autumn–spring storm waves are observed to have peak periods of some 6–10 s with maximum wave heights of about 1.5 m (Boczar-Karakiewicz et al., 2005). In summary, the average, annual significant wave height is 1.0 ± 0.6 m with a mean peak period of 8.3 ± 2.6 s (Lee et al., 1998).

The third experimental site is located on the Mediterranean Sea (Jerba Island, Tunisia). The bathymetry measurements at this site were collected over a period of 10 months (September 1999 to May 2000) along a 9 km stretch of the beach. The mean slope of the nearshore profile up to a water depth of 8 m is quite gentle at about 0.0032. The beach sediment is composed of silica (fine and medium sand, with a mean diameter of about 0.2 mm) and of carbonates (derived from degradation of shells, with diameters of some 0.08 mm). The nearshore-zone sediment lays over bed rock and the thickness of the sand layer is non-uniform, varying in the on–offshore direction from some 1.5 m in the very nearshore to 0 in water depth of 8 m. The wave climate, which is typical for the Southern part of the Mediterranean Sea, is comprised of waves with periods up to 14 s and corresponding wave heights of 3.5 m (Boczar-Karakiewicz et al., 2001). The frequent storm waves have significant energy in periods in the range of 5–9 s with wave heights over 1.3 m.

4. The equilibrium beach profile

Proposed here is a class of shape functions f that can describe both the very nearshore area and the deeper portion of the littoral zone. As mentioned in Section 2, the existing descriptions (5)-(7) are not especially accurate in the onshore portion of the nearshore zone. The idea of splitting the nearshore profile into two parts was explored by Inman et al. (1993), Pruszak et al. (1997) and Larson et al. (1999). In all these papers, the determination of a division point is based on geometrical subjectivity and visual judgment. It is proposed to extend this approach to shape functions in present use with a one-side Taylor expansion around a point x_0 that has already been defined in the existing theories (Pruszak et al., 1997). Of course, the Taylor expansion must be truncated to be of practical use, so in fact this amounts to polynomial approximation. In general, such a scheme would require the determination of too many additional parameters to be of practical interest. However, it will be shown that at least for the three detailed examples described in Section 3, a good representation of an equilibrium profile may be obtained using only a quadratic function for the very nearshore zone and the lower part of the visible beach. Such a representation requires only one further parameter in addition to those already inherent in f.

In earlier work, the prediction of the equilibrium profile was limited to the part of the nearshore zone further from the shore than a certain point x_0. For a barred profile, x_0 was proposed by Pruszak et al. (1997) to be located at the midpoint of the average distance of the inner bar from the shoreline. Preliminary analysis indicates that changing the position of cut-off point x_0 does not significantly impact the fitting errors and, therefore, the calculated parameters. This means that the dividing point between two parts of the profile is not crucial for the method presented here. We will systematically use this method of determining the cut-off point x_0 in all that follows. The calculated values of the distance x_0 is 70 m (profile eta21) and 64 m (profile eta22) for the Gold Coast site obtained with 14 and 18 measured profiles, respectively. For Duck the distance x_0 is 48 m (profile #62) and 39.6 m (profile #188) obtained with 144 and 146 measured profiles, respectively. For Jerba the distance x_0 is 71 m (profile p1) and 69 m (profile p2) obtained from 6 and 12 measured profiles, respectively.

In the case of barless topographies, we propose to determine x_0 as the point midway between the shoreline and the position of the first breaking point of the incident wave. The location of the breaking point may be approximated by the saturation criterion which states that the breaking depth h_0 is given as $h_0=H_0/\gamma$, where H_0 is the wave height at the breaking point and $\gamma \approx 0.78$ is the saturation constant (see CEM, 2001). The wave height H_0 should be representative of the period of time during which the profiles developed. Significant wave height H_{sig} is most commonly used by engineers, which we also adopt. The point x_0 is then determined by the relation $h(x_0)=h_0$, which is well defined for a monotonic beach profile h. Possibly better estimates of breaker depth that depend on the profile slope and wave period were expressed by Weggel (1972) and Komar and Gaughan (1973).

In the following, the offshore portion of an equilibrium profile is calculated using the standard shape functions f by fitting this part of the profile with field data as described in Section 2. The fitting functions f in (5), (6) or (7) have three unknown parameters and are nonlinear in the least squares estimation sense. In actual calculations, we have used a nonlinear fitting technique, the Marquardt–Levenberg method (Ratkowsky, 1983; Press et al., 1992) explained briefly in Appendix B.

As mentioned before, the profile of the lower beach and of the very nearshore zone (which corresponds to the range $x<x_0$) is assumed to be approximated by a second-order polynomial that suitably matches the earlier calculated offshore portion of the profile for $x>x_0$. More precisely, it is proposed to write f in the form

$$f(x)=\begin{cases} f_1(x) & \text{for } x\geq x_0, \\ f_2(x)=P+Q(x_0-x)+R(x_0-x)^2 & \text{for } x<x_0 \end{cases} \tag{8}$$

where f_1 is one of the shape functions described in Section 2 and the coefficients P, Q and R defining f_2 are to be determined. Enforcing that the overall profile is a C^1-function, which seems imminently reasonable, means that P and Q are determined by matching to f_1 at x_0. This leaves R to be specified, which is accomplished by linear least squares fitting with the available data. The parameter R may be related to the mean slope S of the visible beach. Choosing a value $\bar{x}$ of x (a point on the beach) where the angle β of the beach inclination is near the mean, the slope S at that point may be represented in the form

$$S = \tan\beta \cong \frac{df_2}{dx}\bigg|\bar{x} = Q + 2R_e(x_0 - x). \tag{9}$$

This formula allows one to approximate the parameter R in the definition of f_2 as soon as are known S, Q and x_0. Alternatively, once one has determined a value of R, Q and x_0, the mean slope of the visible beach may be predicted. Comparisons between the estimated parameter R_e and the fitting value of R are described in Section 5.

To clarify the procedure, we show how the idea is implemented for specific choices of the deeper-water shape function f_1. Reference to Fig. 1 where the coordinates are depicted may be useful.

4.1. Power function

When using the power function representation (5) in the offshore region, the shape function f of the bed profile is specified by providing f_1 and f_2, where

$$\begin{cases} f_1(x) = -A(x + x_s)^\rho & \text{for } x \geq x_0, \\ f_2(x) = P + Q(x_0 - x) + R(x_0 - x)^2 & \text{for } x < x_0, \end{cases} \tag{10}$$

The three parameters A, ρ and x_s are determined more or less as Dean (1991) and Larson (1991) envisioned, from the existing underwater topographical data using the aforementioned nonlinear least squares technique. Once these constants are in hand, P and Q are determined by the smoothness requirement on f at the point x_0, viz.

$$\begin{cases} P = -f_1(x_0) = -A(x_0 + x_s)^\rho \\ Q = f_1'(x_0) = \rho A(x_0 + x_s)^{\rho - 1}. \end{cases} \tag{11}$$

The remaining coefficient R in Eq. (10) is then obtained from a linear least squares calculation using the available topographical data in the domain $x \geq x_0$.

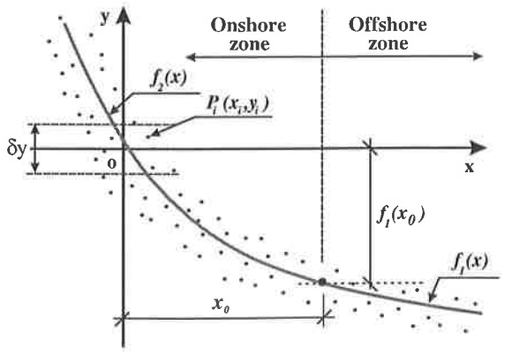

Fig. 1. Scheme of the coordinate system.

4.2. Exponential and logarithmic function

The general forms of the exponential (6) and logarithmic (7) equilibrium profiles are obtained following the approach just described for the power function representation. The equations describing the equilibrium profile f in the entire nearshore zone including the lower part of the beach for the exponential profile are

$$\begin{cases} f_1(x) = -B\left(1 - e^{-kx+C}\right) & \text{for } x \geq x_0, \\ f_2(x) = -B\left(1 - e^{kx_0+C}\right) + Bke^{-kx_0+C}(x_0 - x) + R(x_0 - x)^2 & \text{for } x < x_0. \end{cases} \tag{12}$$

The logarithmic scheme yields the representation

$$\begin{cases} f_1(x) = -D - \frac{1}{F}\ln\left(\frac{x}{G} + 1\right) & \text{for } x \geq x_0, \\ f_2(x) = -D - \frac{1}{F}\ln\left(\frac{x_0}{G} + 1\right) + \frac{1}{F(x_0+G)}(x_0 - x) + R(x_0 - x)^2 & \text{for } x < x_0. \end{cases} \tag{13}$$

In the following section, equilibrium profiles are calculated for the three experimental sites. All three of the standard representations will be used to describe the offshore portion of the nearshore, whereas the very nearshore and lower beach is described by part of a parabola in the manner just indicated.

5. Field application and comparisons

In the calculations of equilibrium profiles, the field data are used for both the estimates of the coefficients of the various shape functions and in comparisons of the predicted equilibrium profiles with these obtained from field data. The standard models described in Section 2 and the proposed modified profile representations are not predictive in the strong sense unless the parameters are related to more fundamental aspects of the beach in question. Our purpose here is not to investigate this aspect, but rather to determine the representational power of the modified profile formulations suggested here.

The procedure applied in our calculations is as follows:

(i) The x-axis runs along the mean water level. The location of the origin of the y-axis of the x–y Cartesian coordinate system is fixed by averaging the shoreline data from field measurements as described in detail in Appendix A.
(ii) The three coefficients of the equilibrium profiles f_1 are obtained from the nonlinear best fit calculations described in Section 4 for the various beach data. At this stage of the procedure f_1 is fit to data in the entire submarine domain $y \leq 0$ descried in the x–y Cartesian coordinate system chosen in step (i) (see Tables 1–3).
(iii) Next, the coordinate of the cut-off point x_0 is estimated. At x_0, the previously calculated shape functions f_1 are truncated on the onshore side. The point x_0 then becomes the matching point of f_1 with the onshore portion f_2 of the equilibrium profile. For the three experimental sites, x_0 (see Section 4) was obtained by averaging the midpoint of the observed distance of

Table 1
Power function model's best fit parameters

Site	Profile name	Power function			R (m^{-1})
		A ($m^{1-\rho}$)	ρ	x_s (m)	
Gold Coast, Australia	eta21	0.016	0.990	10.8	1.74×10^{-4}
	eta22	0.048	0.841	17.9	1.24×10^{-4}
Duck, North Carolina, USA	#62	0.099	0.654	42.7	5.01×10^{-4}
	#188	0.087	0.673	45.9	6.56×10^{-4}
Jerba Island, Tunisia	p1	0.272	0.443	0.6	1.79×10^{-4}
	p2	0.341	0.428	−4.0	1.05×10^{-4}

Table 2
Exponential function model's best fit parameters

Site	Profile	Exponential function			R (m^{-1})
		B (m)	k (m^{-1})	C	
Gold Coast, Australia	eta21	103.7	0.16×10^{-3}	-0.82×10^{-2}	1.60×10^{-4}
	eta22	49.6	0.38×10^{-3}	-1.65×10^{-2}	1.46×10^{-4}
Duck, North Carolina, USA	#62	13.9	0.95×10^{-3}	-10.14×10^{-2}	5.34×10^{-4}
	#188	15.2	0.85×10^{-3}	-9.23×10^{-2}	7.03×10^{-4}
Jerba Island, Tunisia	p1	7.7	2.04×10^{-3}	-5.74×10^{-2}	1.37×10^{-4}
	p2	8.2	1.71×10^{-3}	-8.35×10^{-2}	0.80×10^{-4}

the first bar crest from the shoreline position as determined in step (ii).

(iv) The parabola f_2 is now matched with f_1 at x_0. The linear fitting procedure using field data is carried out in the portion $x \le x_0$ of the nearshore. The results of the calculations provide the coefficient R of the shape function f_2. (The values of R for the experimental sites and for the three different choices of shape functions f_1 are shown in Tables 1–3.)

(v) Details of the error calculations are provided next in Table 4.

The equilibrium profiles for the beaches featured here, shown in Figs. 2 and 3, are calculated in the entire nearshore zone using in the offshore portion the three earlier models of the shape function. In the very nearshore and for the beach profile above the mean water level, the equilibrium profiles are described by the parabola that is fitted at its offshore end with the already estimated shape functions. Figs. 2 and 3 present the results of this procedure and allow one to compare the resulting shape functions and actual field data. For Duck (Fig. 2), all three shape functions are nearly identical. A similar result was obtained for the Australian site. For these two sites, the equilibrium profiles were calculated using large field data sets that were collected regularly, at approximately equal time intervals. By contrast, for the Tunisian site, the predictions obtained with the three shape functions are different (Fig. 3). The result just mentioned shows that the logarithmic function provides the best fit with field data for a very gently sloping beach such as the Tunisian site. However, the equilibrium profile for this site was calculated using a comparatively small set of field data spanning a period of only nine months. Therefore, the results should be confirmed by further work.

In the following, we will discuss and compare the performance of the different versions of the equilibrium profiles presented in Section 2 and comprising 2-, 3- and 4-parameter shape functions (the latter presents the modifications for the very nearshore zone and the beach above the mean water level).

The result in Fig. 4, where the power functions provide the equilibrium profiles for the Gold Coast, shows clearly that the 2-parameter shape function does not fit the data points in the whole area of the nearshore zone. A good approximation is provided by the 3-parameter shape function in the offshore

Table 3
Logarithmic function model's best fit parameters

Site	Profile name	Logarithmic function			R (m^{-1})
		G (m)	F (m^{-1})	D (m)	
Gold Coast, Australia	eta21	5623.2	0.011	0.84	1.61×10^{-4}
	eta22	2163.8	0.025	0.79	1.46×10^{-4}
Duck, North Carolina, USA	#62	670.2	0.116	1.29	5.25×10^{-4}
	#188	782.9	0.103	1.30	6.92×10^{-4}
Jerba Island, Tunisia	p1	85.0	0.399	0.10	0.86×10^{-4}
	p2	93.9	0.365	−0.05	0.53×10^{-4}

Table 4
Fitting errors of the different fitting models

Site	Profile name	Location	Power law		Exponential law		Logarithmic law	
			$\eta/\eta_1/\eta_2$	$\epsilon/\epsilon_1/\epsilon_2$	$\eta/\eta_1/\eta_2$	$\epsilon/\epsilon_1/\epsilon_2$	$\eta/\eta_1/\eta_2$	$\epsilon/\epsilon_1/\epsilon_2$
Gold Coast, Australia	eta21	overall	0.1553	0.1197	0.1567	0.1207	0.1570	0.1210
		offshore	0.1970	0.0958	0.1997	0.0971	0.2004	0.0975
		onshore	0.5287	0.5285	0.5289	0.5287	0.5288	0.5287
	eta22	overall	0.1797	0.1360	0.1807	0.1368	0.1811	0.1369
		offshore	0.2245	0.1112	0.2246	0.1112	0.2244	0.1113
		onshore	0.6140	0.6068	0.6241	0.6167	0.6291	0.6205
Duck, North Carolina USA	#62	overall	0.1545	0.0951	0.1546	0.0952	0.1546	0.0952
		offshore	0.1961	0.0689	0.1957	0.0688	0.1959	0.0688
		onshore	0.3749	0.3606	0.3761	0.3618	0.3757	0.3614
	#188	overall	0.1458	0.0888	0.1467	0.0893	0.1465	0.0892
		offshore	0.1896	0.0685	0.1893	0.0684	0.1896	0.0685
		onshore	0.3552	0.3293	0.3612	0.3348	0.3594	0.3332
Jerba Island, Tunisia	p1	overall	0.1659	0.1662	0.1184	0.1186	0.1127	0.1129
		offshore	0.3077	0.1324	0.2088	0.0898	0.1998	0.0860
		onshore	0.5795	0.5646	0.4438	0.4324	0.4195	0.4087
	p2	overall	0.1647	0.0688	0.1217	0.0508	0.1228	0.0513
		offshore	0.2078	0.0558	0.1448	0.0389	0.1494	0.0401
		onshore	0.5665	0.5638	0.4598	0.4575	0.4491	0.4469

portion of the underwater beach but it does not allow a good representation of the beach profile laying above the sea level. The proposed fitting procedure using the 3-parameter power function with the parabola for predicting the equilibrium profile in the very nearshore zone and above the mean water level provides a satisfactory approximation. Similar representations were obtained by applying 2-, 3- and 4-parameter shape functions at Duck and at the Tunisian site.

The exponential and logarithmic functions (2- and 3-parameter) have the ability to estimate the points laying above the sea level. Therefore, comparisons were made using data from the entire nearshore

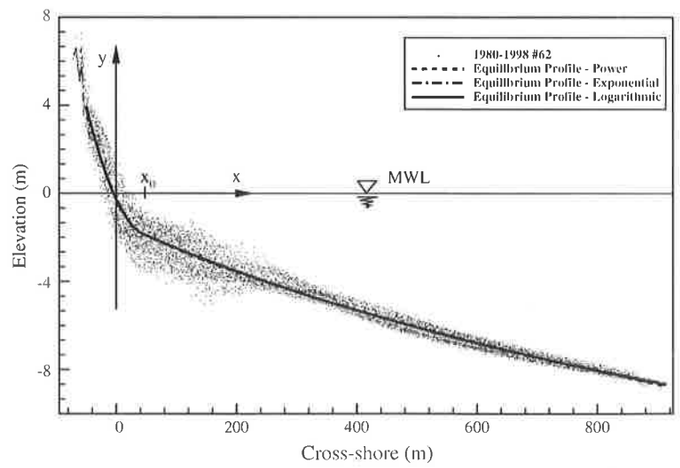

Fig. 2. Foreshore morphology data (profile #62, Duck, NC) (points) represented by the three shape functions.

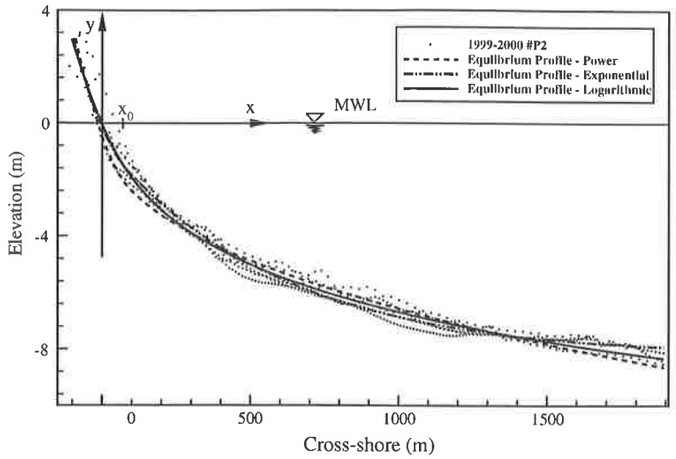

Fig. 3. Foreshore morphology data (profile #2, Jerba Island, Tunisia) (points) represented by the three shape functions.

zone including the visible beach. The different versions of the exponential representations of the equilibrium profile obtained with field data from Duck are presented in Fig. 5. These results show that the 2- and 3-parameter shape function does not fit observations. The 3-parameter shape function fitted with the parabola in the very nearshore and above the mean water level (the 4-parameter approach), represents satisfactorily the equilibrium profile in the entire nearshore zone. Very similar results were obtained by applying the 2-, 3- and 4-parameter shape functions at the Gold Coast site.

To set the stage for quantitative estimation of how well the various shapes functions perform, let $\{(x_i,y_i)\}_{i=1}^{N}$ be determined by the actual bathymetry measurements at one of the sites in question. Here, x_i is the horizontal coordinate at which a bottom elevation y_i was determined. Of course, $y_i>0$ on the visible beach as the measurements are all referred to the mean water level.

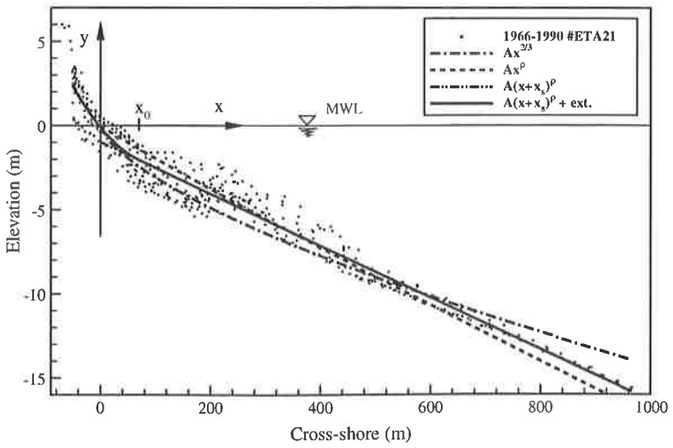

Fig. 4. Foreshore morphology data (profile #eta 21, Gold Coast, Australia) (points) and representation accorded by the four types of power functions.

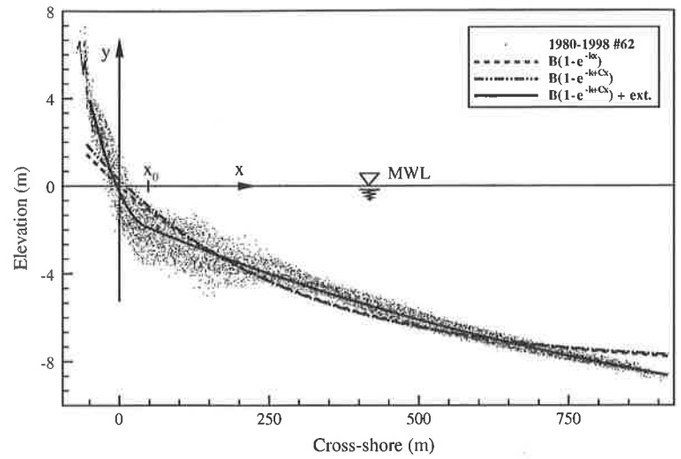

Fig. 5. Foreshore morphology data (profile #62, Duck, NC) (points) and the representation accorded by the three types of exponential functions.

Several goodness of fit measures will be used to estimate how well the various representations match the observations. The first criterion for goodness of fit is

$$\eta^2 = \frac{\sum_{i=1}^{N}(y_i - f(x_i))^2}{\sum_{i=1}^{N}(y_i - \bar{y})^2}, \tag{14}$$

where $\bar{y}$ represents the average of the measured values $\{y_i\}_{i=1}^{N}$. The denominator appearing in Eq. (14) is the root–mean–square of the variation from the mean of the elevation measurements and the values of η indicate the fraction of the variation due to the prediction f. Thus, $\eta=0$ is a perfect fit and η near 1 means the prediction is no better than using the mean value everywhere.

The second overall estimator of the goodness of fit, denoted by ϵ^2, proposed by Bodge (1992), is defined to be

$$\epsilon^2 = \frac{\sum (y_i - f(x_i))^2}{\sum y_i^2}. \tag{15}$$

The value of ϵ is the root–mean–square fraction of the error compared to the overall root mean square value of the elevation measurements. As for η, the value $\epsilon=0$ corresponds to a perfect fit at the measured points.

The error estimators η and ε were first calculated for the entire nearshore zone (overall profile) and then separately for the offshore part (defined by $x_i \geq x_0$), with corresponding errors denoted by η_1 and ε_1, and for the onshore part ($x_i<x_0$) of the nearshore zone, with errors denoted by η_2 and ε_2. The outcomes of these calculations are shown in Table 4.

As was already apparent in Fig. 2 for Duck, the 4-parameter shape functions obtained with the three different presentations for the offshore portion are nearly identical, and consequently, the calculated values of errors are close. A similar result was obtained for the Gold Coast site. The global goodness of fit η and ε for the three shape functions f calculated using field data from the experimental sites are less than 0.16.

However, for the Tunisian site, the 4-parameter power function gives the highest values of η and ϵ. At this site, the average values of the errors, when using the power function, are $\eta=0.1653$ and $\epsilon=0.1175$. The exponential presentation leads to $\eta=0.1201$ and $\epsilon=0.0847$, and the lowest errors, $\eta=0.1178$ and $\epsilon=0.0821$, were obtained when using the logarithmic function. These quantitative results confirm what one gleans from the figures, and indicate that the logarithmic representation of the equilibrium profile better fit data for gently sloping beaches than the other two shape functions. Similar results were obtained in a study of equilibrium profiles at the Catalan Coast (Sierra et al., 1994).

Generally, the errors η_2 and ε_2 corresponding to the prediction f_2 for the onshore part of the nearshore zone are larger than the errors η_1 and ε_1 associated with f_1 for the offshore part. There are several reasons why this might be the case. First, there is less data available for the very nearshore zone than in the offshore portion of the littoral zone. Moreover, the nearshore and beach data are less regularly spaced and have less measured points than the offshore measurements.

The general level of the calculated values of goodness of fit differ among the three experimental field sites. For example, the error η_2 calculated for the Australian site using the 4-parameter approach varies from 0.6291 to 0.5287. By contrast, the same error for the calculated profiles at Duck is 0.3761 and 0.3332, about half that at the Gold Coast site (see Table 4). This is consistent with the assertion that the equilibrium profiles obtained using large and regular sets of field data provide better representations than profiles calculated with a lower and irregular number of observations.

The estimate of the overall errors η and ε for the different types of the calculated equilibrium profiles (1-, 2-, 3-, and 4-parameter fitting functions) representing the entire nearshore zone are presented in Table 5. Calculations for the points lying below the mean water level ($y \leq 0$) are presented for all three type of shape functions. All data points (including the beach above the mean water level) were considered for the exponential and logarithmic shape functions. The calculated errors are significantly lower at all three experimental sites when using the proposed 4-parameter representation than with the existing approaches as might be expected due to the greater number of fitting parameters.

It is noteworthy, and consistent with Larson's earlier conclusions, (Larson, 1991) that the approximation error decreases when the origin of the curve f_1 is allowed to shift along the x-axis. That is, the appearance of the parameters x_s, C, and D significantly improves the shape functions' ability to approximate the measured bed profile. The values of x_s, C and D associated with f_1 for the equilibrium profiles at the experimental sites are shown in Tables 1–3.

The calculated values of the coefficients of the three equilibrium profiles f_1 are now used to estimate corresponding local sediment characteristics and wave parameters by considerations proposed in some of the earlier works mentioned in the Introduction.

The mean values of the coefficient A of Dean's power function (5) increases gradually with the decreasing slopes of the experimental sites. These values are, for the Gold Coast $A=0.049$, for Duck $A=0.093$, and for Jerba $A=0.307$. The mean value of the coefficient ρ decreases with decreasing mean slopes at these sites. The values of ρ are $\rho=0.89$, $\rho=0.66$ and $\rho=0.44$, respectively. It is worth noting an inherent aspect of the power function (5) is that large values of ρ are associated with small values of A and vice versa. This is one of the reasons why, in some findings, the parameter ρ was treated as a constant value (e.g. Dean, 1977, 1991).

The relation between A, the sediment grain size and the fall velocity as proposed by Dean (1991) and Kriebel et al. (1991) is made for profiles with coefficient $\rho=2/3$ and leads to a prediction of the median grain size. Only Duck had ρ near 2/3. The calculated median grain-size diameter $D_{50}=0.15$ mm is just what is observed at this site.

For the three sites under discussion, the mean values of the coefficient k in the exponential representation (5) are $k=0.22\times10^{-3}$ m^{-1} for the Australian coast, $k=0.90\times10^{-3}$ m^{-1} for Duck and $k=1.88\times10^{-3}$ m^{-1} for the Tunisian site. According to the theory, the coefficient k in the shape function f_1 provides an estimate of the mean slope of the nearshore zone. The calculated mean values of k correctly represents the trend in the observed mean geometry of these sites, which is to say the decreasing steepness of their mean nearshore profiles.

The mean values of the coefficient F in the equilibrium profile f_1 of the logarithmic representation (7) are $F=0.015$, $F=0.110$, and $F=0.382$ for the Australian, American and Tunisian sites, respectively. The corresponding mean wave periods deduced from these values of F are $T=16.4$ s, $T=6.0$ s, and $T=3.2$ s. These values are not bad renditions of the observed mean wave periods at the experimental sites (see Section 3).

Generally, although the best fit parameters for neighbouring cross-shore lines at the sites analyzed are a bit different, global similarity is observed. Discrepancies between parameters for each site depend on many factors. For example, in the topographies for the two extremities (profiles #62 and #188

Table 5
Model's overall fitting errors for different variants of shape functions

Function	Number of parameters	Profile	For $y\leq0$		Overall	
			η	ϵ	η	ϵ
$Ax^{2/3}$	1	eta22	0.2372	0.1363	–	–
		#62	0.2499	0.1015	–	–
		p2	0.4232	0.1344	–	–
$A(x+x_s)^{2/3}$	2	eta22	0.2184	0.1329	–	–
		#62	0.1935	0.0786	–	–
		p2	0.3106	0.0987	–	–
Ax^{ρ}	2	eta22	0.1805	0.1099	–	–
		#62	0.2376	0.0964	–	–
		p2	0.2626	0.0834	–	–
$A(x+x_s)^{\rho}$	3	eta22	0.1549	0.0943	–	–
		#62	0.1510	0.0800	–	–
		p2	0.1910	0.0607	–	–
$A(x+x_s)^{\rho}$+ext.	4	eta22	0.1526	0.0943	0.1797	0.1360
		#62	0.1510	0.0800	0.1545	0.0951
		p2	0.1567	0.0603	0.1647	0.0688
$B(1-e^{-kx})$	2	eta22	0.1758	0.1070	0.1744	0.1243
		#62	0.2901	0.1178	0.2679	0.1617
		p2	0.1539	0.0489	0.1417	0.0582
$B(1-e^{-kx+C})$	3	eta22	0.1564	0.0952	0.1736	0.1237
		#62	0.1946	0.0790	0.2633	0.1589
		p2	0.1321	0.0420	0.1417	0.0582
$B(1-e^{-kx+C})$+ext.	4	eta22	0.1540	0.0951	0.1611	0.1155
		#62	0.1497	0.0793	0.1546	0.0952
		p2	0.1095	0.0421	0.1217	0.0508
$1/F\ \ln(x/G+1)$	2	eta22	0.1723	0.1049	0.1711	0.1220
		#62	0.2562	0.1040	0.2025	0.1222
		p2	0.1379	0.0438	0.1456	0.0598
$D+1/F\ \ln(x/G+1)$	3	eta22	0.1563	0.0951	0.1708	0.1218
		#62	0.1943	0.0789	0.2007	0.1211
		p2	0.1379	0.0438	0.1380	0.0567
$D+1/F\ \ln(x/G+1)+ext.$	4	eta22	0.1539	0.0950	0.1608	0.1153
		#62	0.1502	0.0796	0.1546	0.0952
		p2	0.1135	0.0437	0.1228	0.0513

which are more than 1 km apart) at the Duck site, the measured area deformations of the profiles are sometimes significantly different (see Larson and Kraus, 1994; Lee et al., 1998). Variable wave direction and the pier in the middle of the observation area are the major causes of this discrepancy (see Elgar et al., 2001). Additionally, surveys of neighbouring lines were sometimes delayed (1 or 2 days). The distance between profiles at the Gold Coast site is nearly the same (1 km), but the temporal irregularity of the surveys is significant. Moreover, missing profiles at both sites create an unequal number of profiles, another source of variability in the estimated parameters. In contrast, at the Tunisian site, the distance between neighbouring profiles (about 4 km) is the major factor among those already cited that created differences between the fitting parameters.

In the analysis of the onshore parameter R used in Eqs. (10)-(13) and its correlation with measured mean slope S of the visible beach, some individual profiles were used. From the available database, profiles with different slopes were chosen. The steepest beach slope of 0.15 was at the Duck site while the gentlest slope of 0.034 was observed at the Tunisian site. The fitted and estimated results are shown in Table 6, and comparisons between measured and approximated profiles are depicted in Fig. 6. The

Table 6
Power function onshore model's best fit parameters, fitting errors and estimated parameters for chosen individual profiles

Profile	Survey	Function	Function parameters				Overall errors		Estimation		
			A ($m^{1-\rho}$)	ρ	x_s (m)	R (m^{-1})	η	ε	x_0	S	R_e (m^{-1})
#62	02/04/1984	$Ax^{2/3}$+ext.	0.096	2/3	–	5.35×10^{-4}	0.1828	0.1254	57.0	0.150	8.41×10^{-4}
		$A(x+x_s)^{\rho}$+ext.	0.072	0.697	75.7	6.97×10^{-4}	0.1446	0.0991			
#62	10/08/1992	$Ax^{2/3}$+ext.	0.095	2/3	–	4.14×10^{-4}	0.0719	0.0504	38.5	0.073	3.80×10^{-4}
		$A(x+x_s)^{\rho}$+ext.	0.159	0.585	2.9	4.37×10^{-4}	0.0485	0.0340			
eta22	03/11/1988	$Ax^{2/3}$+ext.	0.1432	2/3	–	1.09×10^{-4}	0.2016	0.1398	72.0	0.050	1.76×10^{-4}
		$A(x+x_s)^{\rho}$+ext.	0.081	0.768	6.7	1.31×10^{-4}	0.0737	0.0575			
p2	05/11/1999	$Ax^{2/3}$+ext.	0.063	2/3	–	0.78×10^{-4}	0.3536	0.1420	96.0	0.034	1.03×10^{-4}
		$A(x+x_s)^{\rho}$+ext.	0.433	0.394	−6.5	1.29×10^{-4}	0.1143	0.0459			

analysis presented is limited to the power type function because exponential and logarithmic laws give similar results for the upper part of the beach. Table 6 reports that the values of parameter R obtained by the fitting procedure and of parameter R_e calculated via Eq. (9) are similar. Only for the steepest beach slope is the estimated value R_e slightly greater than R.

To predict equilibrium beach profiles as simply as possible, the full 4-parameter equations need to be reduced. The simplest form of the equilibrium profile of the full Eqs. (10)-(13) can be obtained by neglecting some parameters. In the case of the power type function, Eq. (10) can be reduced to

$$\begin{cases} f_1(x) = -Ax^{2/3} & \text{for } x \geq x_0, \\ f_2(x) = -Ax_0^{2/3} + \frac{2}{3}Ax_0^{-2/3} + R(x_0 - x)^2 & \text{for } x < x_0. \end{cases} \tag{16}$$

Approximation errors for the reduced Eq. (16) is, as expected, worse than for the full Eq. (10) (see Table 6), but can be calculated knowing only three quantities: granularity characterizing the offshore part of the profile (parameter A), the dividing point x_0, and mean slope of the visible beach S. Only for the Tunisian site (the most gentle offshore profile of the sites analyzed) is the 2-parameter function (16) significantly worse than the 4-parameter function (see Fig. 6d). This is because the power law is less capable of estimating gentle offshore profiles than exponential and logarithmic laws (see Table 4 and Fig. 3). As expected, the best fit parameters obtained from individual profiles are different from those that take into account all available surveys for a selected measured line. However, major parameters (e.g., A and ρ) are similar.

6. Conclusions and further discussion

Theory connected with the prediction of equilibrium beach profiles has revolved around specification of a several-parameter family of shape functions, and the further determination of these parameters relative to a specific site. The determination of the parameters has been made by fitting data and by attempts to relate them to other measurable quantities at the nearshore zone in question. Three classes of shape functions in the literature have been identified in the present paper.

Predictions using these classes of shape functions are reasonably accurate in the deeper part of the nearshore zone. The fit is not as good in shallow water, say on the order of 2 m, and in the nearshore portion of the beach.

In an attempt to provide a better descriptive mechanism, we here proposed a new class of shape functions defined piecewise around a point x_0 at a certain distance from the water line. In deeper water, we maintain one of the existing class of shape functions with parameters determined one way or another from field data. This description is held valid for $x \geq x_0$, and for $x \leq x_0$ the simple expedient of matching as well as possible with a parabola is used. Requiring the overall profile to be continuously differentiable means that there is but one further parameter, here called R, to be determined.

This descriptive scheme is tested on bottom profile data at sites in Australia, North America and Africa. This method proves to be considerably superior to the existing methodology. In consequence, we provisionally propose this approach.

Further research is needed to determine the robustness of the described scheme. It is also important to correlate the new parameter R with morphological aspects of the nearshore zone and the prevailing tidal and wave environment. Preliminary analysis indicates that R is related to the mean slope of the visible beach. However, further research could lead to the relationship of R with sediment characteristics in the swash zone.

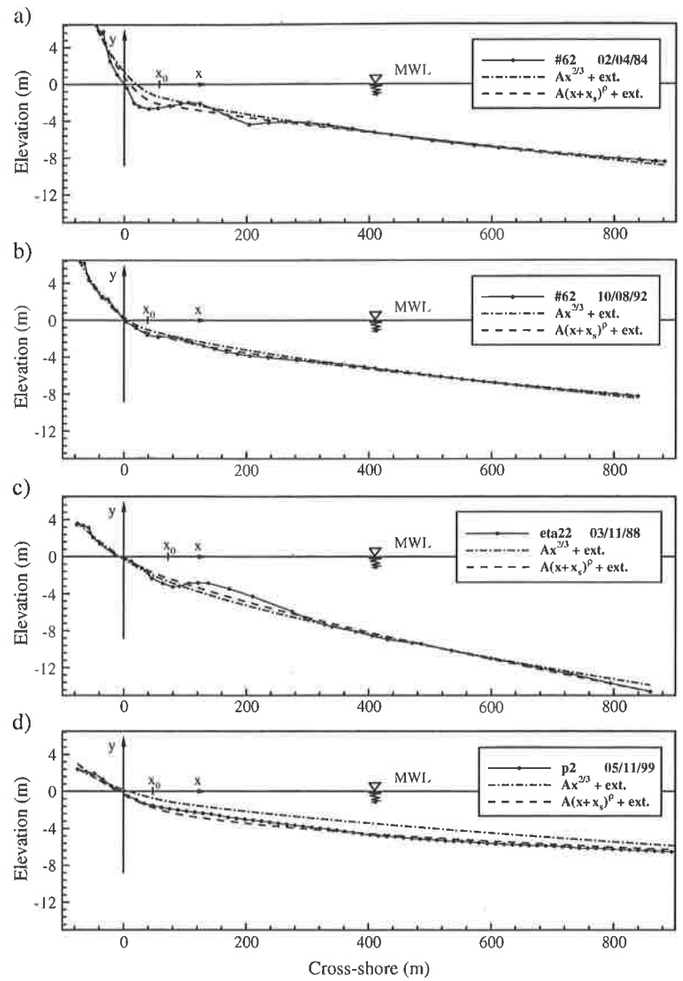

Fig. 6. Comparison of measured and fitted curves represented by the modified 4-parameter power function (10) and the 2-parameter power function (16): (a) and (b) Duck, NC; (c) Gold Coast, Australia; (d) Jerba Island, Tunisia.

Acknowledgements

The authors gratefully acknowledge financial support provided by the National Science Foundation of the USA in a program of Focused Research Groups in

the Mathematical Science. We thank the reviewers of this paper (Dr. John R.-C. Hsu and two anonymous referees) for helpful comments that very considerably improved it. We also appreciate remarks of Dr. E. Thornton on an early draft.

Appendix A. Sea level and shoreline position

It is essential to know the position of the water level in determining the equilibrium beach profile. Measurements of beach profiles are usually referenced to local geodesic data that is the best fit of the geoid to surface data taken at various periods in the past. Naturally, this ignores any change in the mean sea level that occurred later (e.g., for the coasts of the United States and Canada, the most common datum used for land surveys is National Geodetic Vertical Datum (NGVD) of 1929). As the measured changes in mean sea level (MSL) in recent years are relatively small, the differences compared to the geodesic datum is probably negligible. For example, at Duck, the recent average water elevation data is only 8 cm above the MSL during the period 1981–1993 (see Nicholls, 1998). However, in cases where the geodesic data is far from the current MSL, it has to be corrected. The correction involves changing the y-axis elevation and determining a new zero point of the x-axis that represents the actual MSL.

Under the action of waves, wind and tides, the temporal changes of a beach topography can be significant. Generally, the exact location of the coastline over a period of time is unknown. To approximate the shoreline position, we propose to calculate the average horizontal coordinate x_i from available measurement points (x_i, y_i) in the interval for which $-1/2\delta y \le y_i \le 1/2\delta y$. The quantity δy is half of the distance between mean high-water level and mean low-water level. The coastline position thereby determined is the origin of the (x,y) Cartesian coordinate system in which the equilibrium beach profile has been described in this paper.

Appendix B. Curve-fitting procedure

Additional details of the fitting technique used to obtain the three parameters in the offshore descriptive function f_1 are provided here, where f_1 is any of the three previously described shape functions. To obtain f_1 from the data, we apply the Levenberg–Marquardt method (Ratkowsky, 1983; Press et al., 1992), a nonlinear fitting procedure, to determine the three parameters inherent in f_1. In practice, nonlinear least squares is accomplished by iteration rather than solving a linear system of equations as appears in ordinary least squares techniques. Generally, a nonlinear regression model has the form

$$y_i = \mathcal{F}(\boldsymbol{x}_i, \boldsymbol{\theta}) + \beta_i, \qquad i = 1, \ldots, n \tag{B.1}$$

where the y_i are observations, $\mathcal{F}$ is a known function of a vector $\boldsymbol{x}_i = (x_{i1}, \ldots, x_{ik})$ and a parameter vector $\boldsymbol{\theta} = (\theta_1, \ldots, \theta_p)$. The quantity β_i connotes the values of random errors and n, k and p are the number of observations, number of predictor variables and number of parameters, respectively. The errors β_i are usually assumed to be uncorrelated with mean zero and constant variance.The unknown parameter vector $\boldsymbol{\theta}$ in the nonlinear regression model (B.1) is estimated from the data by minimizing the sum of squared residuals

$$\sum_{i=1}^{n} [y_i - \mathcal{F}(\boldsymbol{x}_i, \boldsymbol{\theta})]^2 \tag{B.2}$$

with respect to $\boldsymbol{\theta}$. The resulting estimation obtained from this procedure is called the nonlinear least squares fit.

If the distribution of the errors β_i in Eq. (B.1) is normal, then the least squares estimator for $\boldsymbol{\theta}$ is also a maximum likelihood estimator. Except for a few very special cases, nonlinear regression estimates must be computed by iteration using optimization methods to minimize the error in the goodness-of-fit expression (B.2).

The iteration proposed by Levenberg–Marquardt provides good results in practical applications and has consequently become a standard method in nonlinear least squares analysis. The iterative procedure can be briefly described as follows. If the function $\mathcal{F}$ is continuously differentiable then $\mathcal{F}$ can be linearized locally according to

$$\mathcal{F}(\boldsymbol{x}, \boldsymbol{\theta}) = \mathcal{F}(\boldsymbol{x}, \boldsymbol{\theta}_l) + \mathbf{X}_l(\boldsymbol{\theta} - \boldsymbol{\theta}_l) \tag{B.3}$$

where $\mathbf{X}_l$ is an $n \times p$ matrix with elements

$$\mathbf{X}_l = \frac{\partial \mathcal{F}(\boldsymbol{x}_i, \boldsymbol{\theta}_l)}{\partial \boldsymbol{\theta}_j}. \tag{B.4}$$

Solving Eq. (B.3) for $\boldsymbol{\theta}$ leads to the Levenberg–Marquardt algorithm

$$\boldsymbol{\theta}_{l+1} = \boldsymbol{\theta}_l + \left(\mathbf{X}_l^T \mathbf{X}_l + \lambda \mathbf{D}\right)^{-1} \mathbf{X}_l^T \boldsymbol{e}, \qquad l = 1, 2, 3, \ldots \tag{B.5}$$

which provides a solution when the weighting factor λ is sufficiently large. The vector $\boldsymbol{e}$ represents the residuals $y_i - \mathcal{F}(\boldsymbol{x}_i, \boldsymbol{\theta}_l)$ and the matrix $\mathbf{D}$ in Eq. (B.5) is usually chosen to be either the diagonal part of $\mathbf{X}_l^T \mathbf{X}_l$ or an identity matrix. In either case, it is positive definite of course. In applications, the value of λ is increased as necessary to ensure a reduction in the sum of squares at each internal iteration and is decreased as the sum of the squares of the residuals Eq. (B.2) and the parameters θ converge.

In applications this procedure converges to a solution for well chosen initial values of the parameters. By contrast, the procedure may diverge when these parameters are poorly chosen. Another practical problem is that poorly chosen initial values of the unknown parameters may also cause an erroneous convergence of the procedure to a local minimum rather than toward the global minimum of the least squares problem. When used on the relatively simple problems of interest here, we had very good experience with this procedure.

In the case of the power-law shape function f_1, the starting points were estimated from the linear version of that function (see, Eq. (2)). For the exponential and logarithmic shape functions, there is no associated linear version. Instead, initial values were taken from averaged values reported in the literature (see Section 2).

It is worth mentioning that the nonlinear least squares procedure is sensitive to outliers in the input data. Just as in linear least squares, the presence of one or two outliers in the data can significantly change the results of the nonlinear analysis.

References

Birkemeier, W.A., 1984. Time scales of nearshore profile changes. Proc. 19th Int. Conf. Coastal Eng., vol. II. ASCE, Houston, Texas, USA, pp. 1507–1521.

Boczar-Karakiewicz, B., Jackson, L.A., 1990. The analysis and role of bars in the protection of a beach system: Gold Coast, Queensland, Australia. Proc. 22th Int. Conf. Coastal Eng., vol. III. ASCE, Delft, Netherlands, pp. 2265–2278.

Boczar-Karakiewicz, B., Romańczyk, W., Long, B., 2001. Réhabilitation du littoral par rechargement: Nord-Est de Jerba, Tunisie. Proc. Canadian Coastal Conf. Can. Coastal Science Eng. Ass., Québec, Canada, pp. 13–25.

Boczar-Karakiewicz, B., Romanczyk, W., Bona, J.L., Thornton, E.B., 2005. Seasonal and interseasonal variability of sand bars at Duck, NC, U.S.A. Observations and model predictions, in revision.

Bodge, K.R., 1992. Representing equilibrium beach profiles with an exponential expression. J. Coast. Res. 8 (1), 47–55.

Bruun, P., 1954. Coastal erosion and development of beach profiles. U.S. Army Beach Erosion Board Technical Memorandum 44, U.S. Army Corps of Engineers, Waterways Experiment Station, Vicksburg, Mississippi, USA.

CEM, 2001. Coastal Engineering Manual. U.S. Army Corps of Engineers, Washington, DC.

Dean, R.G., 1977. Equilibrium beach profiles: U.S. Atlantic and Gulf coasts. Ocean Engineering Report, vol. 12. Department of Civil Engineering, University of Delaware, Newark, Delaware, USA.

Dean, R.G. 1990. Equilibrium beach profiles: characteristics and applications. Report UFL/COEL-90/001. Coastal and Oceanographic Engineering Department, University of Florida, Florida, Gainesville, USA.

Dean, R.G., 1991. Equilibrium beach profiles: characteristics and applications. J. Coast. Res. 7 (1), 53–84.

DHL, 1970. Gold Coast, Queensland Australia — coastal erosion and related problems. Tech. Rep. R257, vol. 1–2. Delft Hydraulics Laboratory, Delft, Netherlands.

Elgar, S., Guza, R.T., O'Reilly, W.C., Raubenheimer, B., Herbers, T.H.C., 2001. Wave energy and direction observed near a pier. J. Waterw, Port, Coast., Ocean Eng. 127 (1), 2–6.

Everts, C.H., 1978. Geometry of profiles across inner continental shelves of the Atlantic and Gulf coasts of the United States. Technical Paper, vol. 78-4. U.S. Army Corps of Engineers, Coastal Engineering Research Center, Fort Belvoir, VA, USA.

Fenneman, N.M., 1902. Development of the profile of equilibrium of the sub-aqueous shore terrace. J. Geol. 6 (4), 532–545.

Gold Coast City Council, 1990. Coastal Engineering Works, internal report, Queensland, Australia.

Inman, D.L., Elwany, M.H.S., Jenkins, S.A., 1993. Shorerise and bar–berm profiles on ocean beaches. J. Geophys. Res. 98 (C10), 11,181–18,199.

Kabiling, M.B., Sato, S., 1993. Two-dimensional nonlinear dispersive wave–current and three-dimensional beach deformation model. Coast. Eng. Jpn. 36 (2), 195–212.

Kit, E., Pelinovsky, E., 1998. Dynamical models for cross-shore transport and equilibrium bottom profiles. J. Waterw., Port, Coast., Ocean Eng. 124 (3), 138–146.

Kobayashi, N., 1982. Sediment transport on a gentle slope due to waves. J. Waterw., Port, Coast., Ocean Eng. 108, 254–271.

Kobayashi, N., 1987. Analytical solution for dune erosion by storms. J. Waterw., Port, Coast., Ocean Eng. 113 (4), 401–418.

Komar, P.D., 1998. Beach Processes and Sedimentation. Prentice-Hall, New Jersey, USA.

Komar, P.D., Gaughan, M.K., 1973. Airy wave theory and breaker height prediction. Proc. 13th Int. Conf. Coastal Eng. ASCE, Vancouver, Canada, pp. 405–418.

Komar, P.D., McDougal, W.G., 1994. The analysis of exponential beach profiles. J. Coast. Res. 10 (1), 59–69.
Kriebel, D.L., Kraus, N.C., Larson, M., 1991. Engineering methods for predicting beach profile response. Proc. Int. Conf. Coastal Sediments '91. ASCE, Seattle, USA, pp. 557–571.
Larson, M., 1991. Equilibrium profile of a beach with varying grain size. Proc. Int. Conf. Coastal Sediments '91. ASCE, Seattle, USA, pp. 905–919.
Larson, M., Kraus, N.C., 1994. Temporal and spatial scales of beach profile change, Duck, North Carolina, USA. Mar. Geol. 117, 75–94.
Larson, M., Kraus, N.C., Wise, R.A., 1999. Equilibrium beach profiles under breaking and non-breaking waves. Coast. Eng. 36, 59–85.
Lee, G.-H., Nicholls, R.J., Birkemeier, W.A., 1998. Storm-driven variability of the beach-nearshore profile at Duck, North Caroline, USA, 1981–1991. Mar. Geol. 148, 163–177.
Lee, P.Z.-F., 1994. The submarine equilibrium profile: a physical model. J. Coast. Res. 10 (1), 1–17.
Lippman, T.C., Holman, R.A., Hathaway, H.H., 1993. Episodic, nonstationary behavior of a double bar system at Duck, North Carolina, U.S.A., 1986–1991. J. Coast. Res. 15, 49–75 (Special Issue).
McGrath, B.L., Patterson, D.C., 1972. Wave climate at Gold Coast, Queensland. 8 Div Tech. Papers, vol. 13(5). Institute of Engineering in Australia, Queensland, Australia.
Nicholls, R.J., 1998. Evaluation of depth of closure using data from Duck, NC, USA. Mar. Geol. 148, 179–201.
Press, W.H., Teukolsky, S.A., Vetterling, W.T., Flannery, B.P., 1992. Numerical Recipes in Fortran 77. Cambridge University Press, New York, USA.
Pruszak, Z., Różyński, G., Zeidler, R.B., 1997. Statistical properties of multiple bars. Coast. Eng. 31, 263–280.
Ratkowsky, D.A., 1983. Nonlinear Regression Modeling, a Unified Practical Approach. Marcel Dekker, New York, USA.
Roelvink, J.A., Broker, I., 1993. Cross-shore profile models. Coast. Eng. 21, 163–191.
Romańczyk, W., Boczar-Karakiewicz, B., Thornton, E.B., Bona, J.L., 1999. Sand bars at Duck, NC, USA. Observation and model predictions. Proc. of the 4th Int. Conf. Coastal Sediments '99. ASCE, New York, USA, pp. 491–504.
Sierra, J.P., Lo Presti, A., Sánchez-Arcilla, A., 1994. Equilibrium beach profiles on the Catalan coast. Proc. Int. Conf. Coastal Dynamics. ASCE, Barcelona, Spain, pp. 432–445.
Silvester, R., Hsu, J.R.C., 1997. Coastal stabilization. Advanced Series in Ocean Engineering, vol. 14. World Scientific, Singapore.
Smith, A.W., Jackson, L.A., 1990. Assessment of the past extent of cyclone beach erosion. J. Coast. Res. 6 (1), 73–86.
van Rijn, L.C., 1998. Principles of Coastal Morphology. Aqua Publications, Amsterdam.
Watanabe, A., 1982. Numerical models of nearshore currents and beach deformation. Coast. Eng. Jpn. 25, 147–161.
Weggel, J.R., 1972. Maximum breaker height. J. Waterw., Port, Coast., Ocean Eng. 98 (4), 529–548.
Work, P.A., Dean, R.G., 1991. Effect of varying sediment size on equilibrium beach profiles. Proc. Int. Conf. Coastal Sediments '91. ASCE, Seattle, USA, pp. 890–904.